Comparison of Terahertz, Microwave, and Laser Power Beaming Under Clear and Adverse Weather Conditions

Lou Rizzo, John F. Federici, Samuel Gatley, Ian Gatley, James L. Zunino & Kate J. Duncan

Journal of Infrared, Millimeter, and Terahertz Waves

ISSN 1866-6892

J Infrared Milli Terahz Waves
DOI 10.1007/s10762-020-00719-w

Springer

Journal of Infrared, Millimeter, and Terahertz Waves
https://doi.org/10.1007/s10762-020-00719-w

Comparison of Terahertz, Microwave, and Laser Power Beaming Under Clear and Adverse Weather Conditions

Lou Rizzo[1] · John F. Federici[1] · Samuel Gatley[1] · Ian Gatley[1] · James L. Zunino[2] · Kate J. Duncan[3]

Received: 17 January 2020 / Accepted: 11 June 2020/Published online: 30 June 2020

Abstract
Wireless transmission of power from point to point has been developed in two predominate electromagnetic frequency ranges: near-infrared and microwave. In this paper, the prospect of wireless power beaming in the terahertz frequency range is explored with emphasis on the role of adverse weather. Link distance, power transmission, and safety performance of near-infrared, microwave, and terahertz power beaming are compared under clear and adverse weather conditions. While infrared power beaming provides the longest link distances of the three under clear weather conditions, terahertz power beaming can provide better performance under adverse weather conditions.

Keywords Power beaming · Terahertz · Attenuation · Weather

1 Introduction

Power beaming is the wireless transmission of electrical power. Typically, electrical power is converted to propagating electromagnetic radiation. After propagating through the atmosphere, the electromagnetic radiation is converted on the receiver end into electrical power. In the optical/near-infrared spectrum (sometimes called laser power beaming (LPB)), a laser is used to generate the electromagnetic radiation while photovoltaics are employed to convert the laser beam to electrical power. At lower frequencies, microwave sources convert electrical power to

✉ John F. Federici
federici@njit.edu

[1] Department of Physics, New Jersey Institute of Technology, 323 Martin Luther King Blvd, Newark, NJ 07102, USA

[2] U.S. Army Combat Capabilities Development Command (CCDC), Armaments Center FCDD-ACM-AP, Picatinny Arsenal, Wharton, NJ 07885, USA

[3] Photonics Research Center, United States Military Academy, West Point, NY 10996, USA

microwave radiation, which is converted back to direct current (DC) electrical power using a rectifying diode and an antenna. Microwave power beaming (MPB) and LPB are far-field means of wireless power transfer, unlike inductive or resonance coupling, which can only transfer power for short-range distances [1].

Applications of interest for power beaming include extended operation of battery-powered remote ground and aerial vehicles under the constraints of battery life. Weight and space restrictions of these vehicles often prohibit the use of larger batteries. Power beaming will allow for the recharging of batteries during vehicle use at extended distances from the operator. Recharging of remote sensors is another application of interest for power beaming. Changing batteries may not be practical for sensors in hazardous locations. Installation of transmission lines can be difficult due to terrain and cost prohibitive in some situations.

Magnetrons are typically used to generate microwaves for MPB. Frequencies of 2 to 5.8 GHz have been employed with kilowatt power output [1, 2]. A rectenna is a rectifying diode attached to an antenna that is typically configured for use as a detector or electrical power converter. The antenna receives the incident electromagnetic radiation, and the rectifying diode coverts the alternating current to direct current for either storage or to power a real-time system.

Raytheon was the first to successfully demonstrate microwave power transmission at 3 GHz in 1963 to power a fan 20 ft away. By October 1964, Raytheon improved their microwave power transmission system, transmitting energy to a 6-ft diameter tethered helicopter with a 4-ft^2 rectenna receiver 60 ft above a transmitting antenna [2]. In 1975, an MPB experiment was conducted at the Venus Site of JPL Goldstone [2]. These trials were conducted at 2.388 GHZ with a 26-m diameter parabolic transmit antenna and a 3.4×7.2-m^2 rectenna array [1]. The microwave power was transmitted at a distance of 1 mile. The overall efficiency of the transferred microwave power was only 6.7%, with 30-kW converted to dc power from a 450-kW emitted beam. Other experiments in 1987 [3] and 1992 [1] demonstrated microwave powering of model planes. In both cases, a 2.45-GHz source was used and the distance between the source and receiver was approximately 10 m. More recently, a MPB system operating at 60 GHz with a 4-cm separation between the source and receiver [4]. As will be discussed later in this paper, the relatively short link distances for MPB can be anticipated both because of significant diffraction (sometimes called "free-space damping") and because of the relatively small receiver areas for microwave power beaming to drones. In order to increase the link distances and reduce the required source power, one needs to use higher frequency sources (e.g. near-infrared or terahertz (THz) sources) to minimize the diffraction (free-space damping) effect.

Some notable LPB applications include a NASA demonstration of a small plane flown indoors in 2003 [5]. EADS Space Transport powered a mini rover by LBP in 2003 [5]. In 2009, Powerlight Technologies (formerly LaserMotive) won the NASA beam power challenge by using an infrared laser to drive a robotic climber up a 900-m cable [6]. Powerlight Technologies has also demonstrated the first outdoor flight powered by LPB with a Stalker unmanned aerial system (UAS) [7].

Terahertz power beaming (THzPB) has lagged in development compared to infrared and microwave due to the immaturity and inefficiencies of the rectifying diodes. However, a recent THz science and technology roadmap [8] for high power sources describes compact sources in the 100–500 GHz range that have been demonstrated with output powers of roughly 1 kW, while 0.4–0.5 THz CW Gyrotrons [9] producing power levels of > 10 kW are also available for THzPB sources. These commercial off-the-shelf sources are more than sufficient for THz

power beaming. To convert the THz power to electrical power will require development and advances of rectifying diodes, which can operate at these frequencies [10]. Development of rectifying diodes in the THz range is an active area of research [11, 12]. One laboratory demonstration of THz power beaming at 303 GHz demonstrated with a conversion efficiency of ~ 2% [13]. This relatively low conversion efficiency at THz frequencies is a technological step towards achieving efficient THzPB performance.

The primary focus of this paper is to address the effects of weather on power beaming and compare microwave, THz, and infrared power beaming under identical atmospheric conditions. Atmospheric attenuation and its impact on power beaming generally have not been studied. A comparative analysis is essential: the three spectral bands will be affected differently due to certain weather conditions. For example, while LPB using infrared lasers has the advantage over long distances in clear weather, fog makes these systems inoperable. Even under clear weather conditions (e.g. indoor PB of drones in a logistics distribution center), water vapor has a profound effect on the propagation distance of THz beams, which not only limits the maximum propagation distance for THz power beaming but also determines the optimal THz frequency for power beaming.

This paper is organized as follows: Sect. 2 discusses laser, microwave, and terahertz hazard fundamentals including maximum permissible exposure (MPE) levels. Section 3 outlines a Gaussian profile beam approach to estimate the received power in a power beaming link as function of distance, frequency, and atmospheric conditions. Power transmission is calculated both for clear weather and in the presence of airborne particulates such as dust, fog, rain, sleet, and snow. In Sect. 4, effects of the spectrally dependent conversion efficiency of the receiver are discussed. Comparison of laser, microwave, and THz power beaming performance and conclusions are summarized in Sect. 5.

2 Safe Operational Limits

A major concern of power beaming is the hazard associated with direct beam exposure from high power laser, microwave, or THz sources. This can be a limiting factor for LBP, restricting its application to specific areas of laser hazard zones and requiring LPB operators to wear personal protection equipment [14]. The standard guide for the safe use of lasers and hazard analysis in industry, research laboratories, and defense programs is ANSI Z136.1-2014 American National Standard for Safe Use of Lasers (https://www.lia.org/). Safe exposure limits of laser radiation will vary depending on the wavelength of operation and are defined by maximum permissible exposure (MPE). MPE is the maximum irradiance (W/cm^2) that represent a zero risk of adverse biological effects [15]. At risk biological tissues include the skin and eyes, with eyes being further subdivided into MPEs for retina and cornea exposure. In this paper, performance of microwave and THz power beaming systems are compared with an LPB system operating at a wavelength of 1.5 μm. This wavelength has a relatively high MPE of 0.1 W/cm^2 for both the eye and skin limits [14].

Hazardous exposure level standards for microwave and THz sources are indicated by the IEEE Std C95.1-2005 standard titled “IEEE Standard for Safety Levels with Respect to Human Exposure to Radio Frequency Electromagnetic Fields, 3 kHz to 300 GHZ” [16] and the IEEE Std C95.3-2002(R2008) “IEEE Recommended Practice for Measurements and Computations of Radio Frequency Electromagnetic Fields with Respect to Human Exposure

to Such Fields, 100 kHz–300 GHz" [17]. For the spectrum of 300 MHz to 300 GHz with continuous waves (CW), the primary concern is adverse health effects from heating [16].

IEEE has established two tiers of exposure limits for MPE: an upper tier, which applies to persons in a controlled environment, and a lower tier with an additional margin of safety for the general public [16]. While a vast body of evidence shows that the upper tier exposures pose no risk of harm, the lower tier exposures recognize public concerns and can be used to address all long-term exposures. The application of MPB will require high power density transmission through free space in a controlled environment with trained personnel, so the focus of MPE assessments will be on the upper tier limits for continuous exposures greater than 6 min. MPE for microwave exposure is given in Table 1. For example, a typical MPB system operating at 2.45 GHz has an MPE of 81 W/m^2, a THzPB system operating at 250 GHz has an MPE of 100 W/m^2, and an LPB system operating at 1.5 μm has an MPE of 1000 W/m^2. It is interesting to note that the MPE for irradiation using 1.5 μm is larger than that for 250 GHz.

3 Gaussian Beam Model

In order to estimate the diameter of a microwave or THz propagating beam, which is delivering power to a target area, standard equations for Gaussian Beam propagation [18] are employed. The lowest-order transverse electromagnetic mode (TEM 00) will mimic a typical beam profile to model power beaming. The beam profile is circularly symmetric perpendicular to the propagation direction with the highest peak intensity in the center.

For simplicity, the minimum beam diameter is assumed to be at the transmitter ($z = 0$). The Gaussian beam width will increase with propagation distance given by

$$W(z) = W_0\sqrt{1 + \left(\frac{z}{z_0}\right)^2} \tag{1}$$

where W_0 is the minimum beam waist at $z = 0$, z is distance of beam propagation measured from the minimum beam waist, and z_0 is the Rayleigh range given by

$$z_0 = \frac{\pi W_0^2}{\lambda} \tag{2}$$

where λ is the electromagnetic wavelength. The Gaussian beam intensity as a function of radius ρ and distance z is given by

$$I(\rho, z) = \frac{2P_o}{\pi W^2(z)} \exp\left[-\frac{2\rho^2}{W^2(z)}\right] \tag{3}$$

Table 1 Hazardous infrared, microwave, and terahertz exposure in irradiance (W/m^2) for long exposures. Note f_m is the frequency in MHz for determining exposure limits

Frequency/wavelength	Power density S (W/m^2)
300 MHz to 3 GHz	f_m/30
3 to 300 GHz	100
1500 nm	1000

where $P_o = I_o \pi W_o^2/2$ is the total beam power and I_o is the peak intensity of the beam. The power incident upon a receiver is calculated by integrating the radial profile of the Gaussian beam over the area of the receiving aperture using

$$P_r(z) = \frac{2P_o}{\pi W^2(z)} \int_0^{\rho_{\max}} \exp\left[-\frac{2\rho^2}{W^2(z)}\right] 2\pi\rho d\rho = P_o\left(1-\exp\left[-\frac{2\rho_{\max}^2}{W^2(z)}\right]\right) \tag{4}$$

where $\rho_{\max}$ is the maximum aperture radius of the receiver. It is worthwhile recalling that $\rho_{\max}$ represents a physical aperture size, while $W(z)$ is the beam diameter parameter of a Gaussian beam. Only ~86% of the power of a Gaussian beam is within a physical radius equal to $W(z)$, while 99% of the power is contained within a physical radius of 1.5 $W(z)$.

3.1 Model Parameters and MPB Analysis

To compare infrared, microwave, and THz power beaming in this paper, it is assumed that 10 W of power is required to be incident on the receiver and the aperture radii of the transmitter and receiver are both 0.5 m, regardless of electromagnetic wavelength. In Sect. 4, effects of the spectrally dependent conversion efficiency of the receiver are discussed. For an aperture radius of 0.5 m, corresponding to 1.5 $W(z)$ the corresponding beam radius for Gaussian optics at the transmitter is W_o= 0.33 m. The Rayleigh ranges (Eq. (2)) for the microwave (2.45 GHz), THz (300 GHz), and infrared (1.5 μm wavelength) beams are given by 2.8 m, 340 m, and 228 km, respectively.

Solutions will be based on a Gaussian beam propagation model Eq. (4) including atmospheric attenuation given by

$$P_r(z) = \varepsilon_d P_o\left(1-\exp\left[-\frac{2\rho_{\max}^2}{W^2(z)}\right]\right) e^{-\alpha_{atm}\ z} \tag{5}$$

where ε_d is the efficiency of the receiver. Clearly, microwaves will suffer severely from diffraction over tens of meters distance, while the large Rayleigh range of the infrared implies that the infrared beam maintains the same beam diameter over an equivalent distance. However, due to relatively low eye and skin exposure MPE levels for infrared light [14], there is an advantage to use a wide infrared beam for beam powering since the lower intensity reduces the safety impact of direct beam exposure.

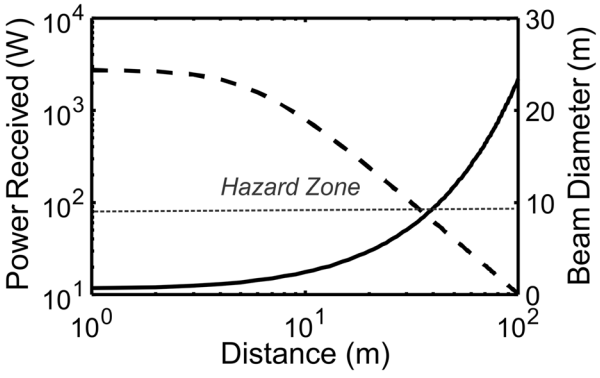

Fig. 1 Power received (dashed line) versus distance (left scale). A 2800-W 2.45 GHz transmitter would be required in order to collect 10.18 W of power at a distance 100 m from the transmitter. The effective area of the receiver is $\pi 0.5^2$ m^2. Beam diameter (solid line) as a function of distance from the transmitter for 2.45 GHz (right scale)

Analysis for an MPB system with $\alpha_{atm} = 0$ at an operating frequency of 2.45 GHz and use of Eq. (5) is shown in Fig. 1. This figure shows that a 2800-W transmitter would be required to receive 10.18 W at 100 m. At this frequency, the rapid beam spreading (large angular divergence) with propagation distance dictates that only a portion of the transmitted beam will illuminate the targeted receiver.

Figure 1 also shows that the required transmitted power would have a hazard zone up to 35 m from the transmitter. At this distance, the peak intensity of the Gaussian beam is 81 W/cm^2, which is at the limit of MPE for microwaves in this frequency range. For the target parameters of 10 W at 100 m distance, sufficiently powerful microwave sources exist at 2.45 GHz, but the process is so inefficient (< 1% efficiency) due to spreading of the power beam that there is a large hazard area.

A hazard free system for short range MPB could be developed at 2.45 GHz frequency with a 78-W transmitter. A total of 10.8 W power would be received at a distance 16 m from the transmitter. The essential point is that diffraction severely limits microwave power beaming over significant distances. A microwave beam spatially spreads quickly with propagation distance essentially wasting power, limiting the maximum range of power beaming, and creating a safety hazard. To circumvent these issues, higher frequency electromagnetic beams—e.g. near-infrared or Terahertz—are needed. However, for these alternative power beaming frequencies, the impact of weather can play a major role.

3.2 Effects of Weather on Power Beaming

Figure 2 compares the absorption coefficient of millimeter waves, THz, and infrared waves at sea level for different weather conditions. In the absence of airborne particulates (e.g. fog or rain), the atmospheric absorption is dominated under clear weather condition by absorption by atmospheric gases, predominately oxygen and water vapor. The atmospheric attenuation may be calculated using the International Telecommunications Union (ITU) standards.

The black dashed line from 10 to 1000 GHz in Fig. 2 indicates the "free-space damping" attenuation $A_r A_t / z^2 \lambda^2$ for a distance of $z = 500$ m and $\pi 0.5^2$ m^2 apertures for both the transmitter $A_t$and receiverA_r. The Gaussian beam has a minimum Gaussian radius given by 0.5/1.5 at the transmitter. The electromagnetic frequency is $\nu = c/\lambda$, where c is the speed of light. For power beaming, the effective power loss between the transmitter and receiver will be the sum of free-space damping and atmospheric attenuation. From the plots of Fig. 2, it is clear that there are two available spectral ranges for power beaming: in the infrared/visible range (for which diffraction or free-space damping is not a concern) and in the THz range from about 100–500 GHz depending on weather conditions, aperture sizes, and propagation distances. In particular, certain spectral "windows" are available for THz power beaming such as the 200–300 GHz window. Since the attenuation varies with frequency even for clear weather conditions, there are two essential considerations for THz power beaming: (a) what is the optimal frequency (or frequency range) for power beaming? (b) What is the maximum range of THz power beaming for various weather conditions?

3.3 Indoor/Clear Weather Propagation

Much of the analysis in the next two sections builds upon our previous work on THz wireless communications in the presence of adverse weather and environmental conditions [19–22]. Starting with the Gaussian Beam formulation given by Eq. (5), one may calculate the total

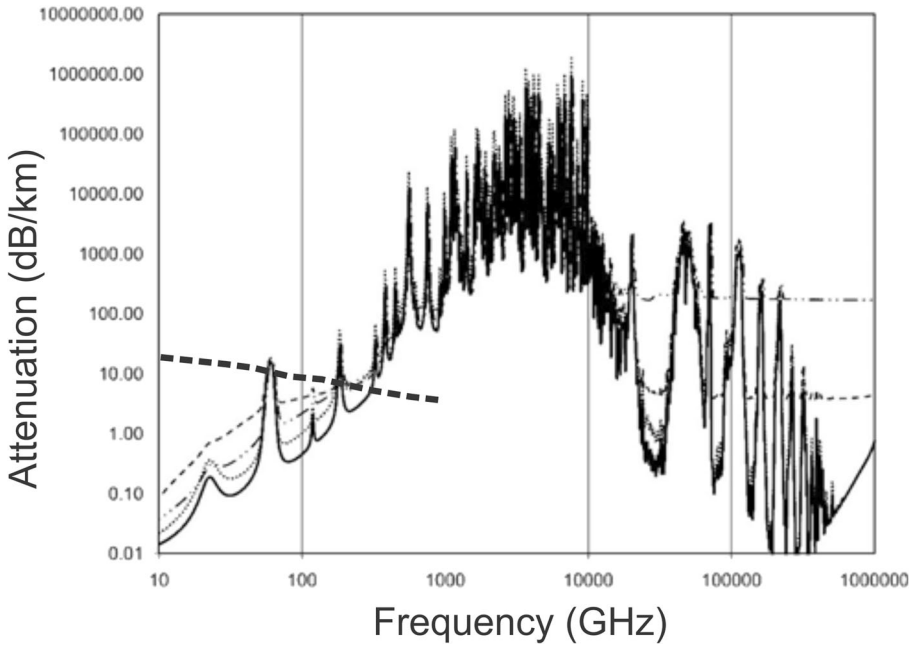

Fig. 2 Calculated atmospheric attenuation in THz and IR band adapted from [19, 20]. The dashed, dash-dot, solid, and dotted lines correspond to 4 mm/h of rain, 100 m visibility of fog, US standard atmospheric conditions at sea level, and 15 g/m^3 of water content, respectively. The long black dashed line corresponds to the expected attenuation due to "free-space damping" for an assumed distance of 500 m with $\pi 0.5^2$ m^2 transmitter and receiver effective areas. The corresponding Gaussian beam radius at the transmitter is 0.33 m. An infrared wavelength of 1.5 μm corresponds to a frequency of 2×10^5 GHz

power incident on a receiving antenna after passing through a clear atmosphere (i.e. no fog, rain, snow, etc.). Under clear weather conditions, the attenuation in the THz range can be calculated using the ITU-R P.676-11 standard [23]. For this standard, the attenuation through atmospheric gases, which is valid from 1 to 1000 GHz, is estimated by a summation of individual absorption lines.

As typical non-winter weather conditions, the following atmospheric conditions are assumed for clear weather: an atmospheric pressure of 1013.25 hPa, temperature of T = 288 K, and water vapor density of 7.5 g/m^3. For this temperature and water vapor density, the relatively humidity (RH) is ~ 59%. As shown in Figs. 3 and 4, the range of THz frequencies for which there is significant received power at the receiver depends on the propagation distance as well as the aperture sizes. For short distances ~ 10 m and aperture radii of 0.25 m, there is high transmission throughout most of the THz range. For mid-range distances (~ 10–50 m), the received power is over 90% for a wide range of THz frequencies between 100 and 300 GHz.

As the propagation distance for THz Beam Powering increases, two effects occur simultaneously: (a) diffraction or free-space damping which decreases the total collected power at the fixed area receiver since the propagating THz energy is spread over a larger area and (b) the atmospheric attenuation becomes more pronounced. At low THz frequencies, the diffraction or "free-space damping" is the dominant effect, while at the higher THz frequencies, the atmospheric attenuation from water vapor has the larger impact. As shown in Fig. 3, the peak

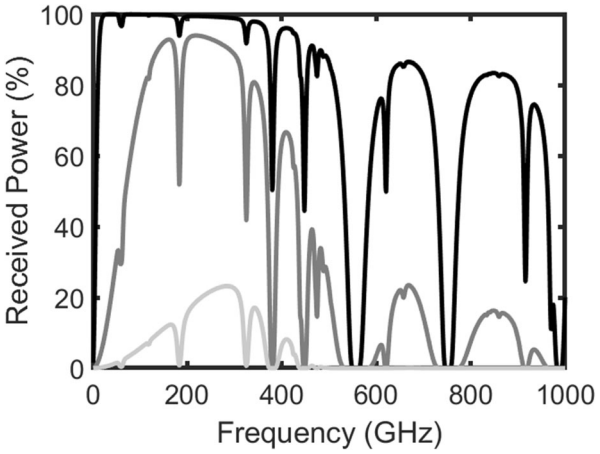

Fig. 3 Percent received power relative to transmitter power for distances of 10 m (black), 100 m (dark gray), and 500 m (light gray). Atmosphere conditions correspond to an atmospheric pressure of 1013.25 hPa, temperature of T = 288 K, and water vapor density of 7.5 g/m^3. The effective radii of the transmitter and receiver are assumed to be 0.25 m

of received power for 100 m propagation distance occurs at ~ 218 GHz. For 500 m, the maximum received power occurs at 284 GHz, but the received power is significantly reduced due to water vapor absorption and diffraction.

While the discussion above shows that the combination of diffraction and atmospheric attenuation determines the optimal frequency for THzPB, one can adjust the optimal frequency by adjusting the aperture sizes for the transmitter and receiver to reduce the effect of diffraction. Figure 4 illustrates the effect of doubling the effect radii of the transmitter and receiver to 0.5 m. For a distance of 100 m, a much broader range of THz frequencies between 100 and 300 GHz yields received power levels above 90%. At a distance of 500 m, the peak of the received power shifts from 284 to 230 GHz, while the received power increases from ~ 24 to ~ 64%.

Under clear weather conditions, the main limitation to THz propagation over 100 GHz in the atmosphere is water vapor. Water vapor plays a significant role in limiting the operational capabilities of THz communication systems [24–26]. Infrared beams should exhibit longer propagation distances due to lower attenuation under clear weather conditions (< 1 dB/km from Fig. 2) as well as a less spreading of the beam due to diffraction (Rayleigh range ~

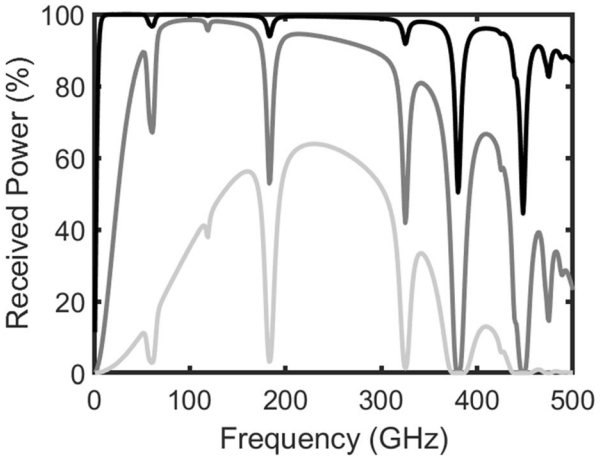

Fig. 4 Percent received power relative to transmitter power for distances of 10 m (black), 100 m (dark gray), and 500 m (light gray). Identical atmospheric conditions to Fig. 3. The effective radii of the transmitter and receiver are assumed to be 0.5 m

228 km). For intermediate distances (~ 100 m) both THz and infrared intensity levels are below minimum MPE levels for safe operation. As shown in Fig. 3, a 218-GHz THzPB system with a 10.6-W transmitter can deliver 10 W on target at a distance of 100 m. The maximum average intensity of the THz beam would be about 54 W/m^2, which according to MPE limits of Table 1 would be within safety limits. A 10-W infrared laser beam operating at 1.5 μm with an equivalent effective area of $\pi\, 0.5^2$ m^2 yields an average intensity of 13 W/m^2, which is both eye- and skin-safe.

3.4 Transmitting Power in Adverse Weather

The impact of airborne particulates on THz and infrared propagation depends fundamentally on the size of the particulates relative to the electromagnetic wavelength. Under dust, fog, rain, etc. conditions, Mie scattering models of the airborne particulates [20–22, 27] are used to predict the atmospheric attenuation. In calculating the attenuation due to airborne particulates, typically one must include the particle size distribution of the particulates in the Mie scattering analysis.

Initially, the effects of dust and fog on THzPB are emphasized. Typically, the wavelength of THz radiation is much larger than the size of these airborne particulates. The attenuation of THz radiation by dust, smoke, and fog is much less severe than in the infrared/optical range. Consequently, LPB may become inoperable, while THzPB would be affected only slightly in these adverse weather conditions.

As an example of the impact of dust on THzPB, the effect of attenuation by bentonite powder [28] is modeled. Bentonite powder is a mixture of clay formed from volcanic ash decomposition and largely composed of montmorillonite and beidellite. The average particle radius is 4.3 μm. The complex refractive index of the bentonite powder is modeled using $\tilde{n}(\nu) = 1.54 + in_i(\nu)$, where the imaginary refractive index is given by

$$n_i(\nu) = \frac{\alpha_q \nu c}{2\pi} \tag{6}$$

where c is the speed of light in a vacuum and α_q is a constant. For this functional form of the imaginary refractive index, the absorption coefficient for solid bentonite given by $\alpha(\nu) = 2\pi\nu\, n_i(\nu)/c$ is a quadratic function of frequency. Using the standard Mie scattering formulation [21, 28], the attenuation coefficient of bentonite dust particles can be calculated. As an example, Fig. 5 shows the expected attenuation coefficient in the THz frequency range for a number density of 6.5×10^9 particles/m^3. A value of $\alpha_q = 3.14 \times 10^{-20}$ s^2/m is used in the simulation so that the predicted attenuation of the dust cloud roughly matches the measured attenuation at 625 GHz from Ref. [28].

Using the calculated attenuation coefficients from Mie scattering for the airborne particulates and the ITU model for attenuation by atmospheric gases, one can calculate the received beam power through dust clouds. As shown in Fig. 6, under clear atmospheric conditions (no dust), significant received power (> 90%) is available from about 100–180 to 200–300 GHz. With a particle density of 6.5×10^8 m^{-3}, the received power essentially is unchanged near 100 GHz and > 80% near 300 GHz. At a particle density an order of magnitude larger, the received power is significant only in a narrow spectral range near 100 GHz. For comparison, at an LPB wavelength of 1.5 μm and a refractive index of 1.5, the attenuation cross-section calculated from Mie scattering is ~ 1.4×10^{-10} m^2. The attenuation coefficient at 1.5 μm for a particle density of 6.5×10^9 m^{-3} would be about 4 dB/m. For a path length of 100 m and dust

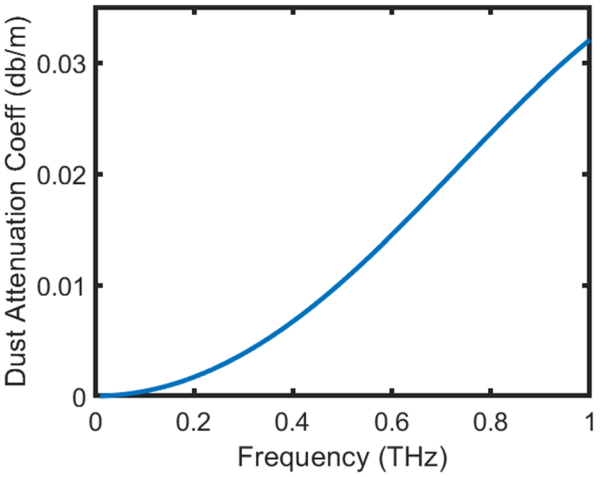

Fig. 5 Calculated attenuation coefficient versus frequency due to bentonite dust. The curve is calculated using a Mie scattering model assuming a real index of 1.54 and an imaginary refractive index of the form given by Eq. (6). The number density of particles is 6.5×10^9 m^{-3}

cloud particle densities of 6.5×10^8 m^{-3} and 6.5×10^9 m^{-3}, the corresponding received power would be ~ 0.02% and essentially zero, respectively. In the presence of dust, a 100-m THzPB link could still be operational, while a LPB link would be completely blocked.

For attenuation by fog, there are two contributions to the net atmospheric attenuation: attenuation by water vapor (typically a relative humidity of 100%) and attenuation by fog droplets. For the first contribution, one can use the ITU standard for attenuation by atmospheric gases evaluated at a temperature and water vapor density consistent with 100% RH. The attenuation calculation by fog droplets may be simplified using Rayleigh's approximation to Mie scattering [25, 29, 30]. In this approximation, the details of the particle size distribution are unimportant (as long as most particles are much smaller than the THz wavelength), and one can replace the particle distribution function with total mass density of fog droplets in the atmosphere. The Rayleigh limit of Mie theory very closely approximates Mie theory predictions up to about 300 GHz [29]. The two approaches agree to within 4% up to 500 GHz and within 14% up to 1000 THz. Since implementations of THzPB will most likely require

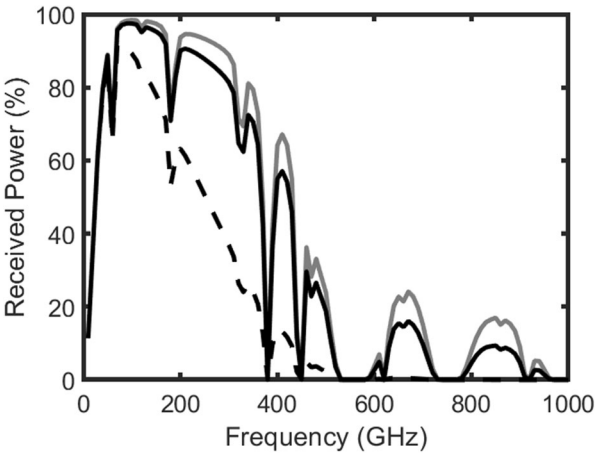

Fig. 6 Received power as a function of frequency through 100 m path length. For all curves, the temperature is 17 °C and the apertures are 0.5 m in radius. The gray curve corresponds to clear weather and 7.5 g/m^3 water vapor. The solid and dashed black lines correspond to 6.5×10^9 particles/m^3 and 6.5×10^8 particles/m^3, respectively, of bentonite dust

frequencies below 500 GHz (due to atmospheric water vapor), then Raleigh's limit of Mie scattering theory is applicable for evaluating the impact of fog.

Typically, fog droplets are approximately 10 μm in size [30]. Since the droplet size is much smaller than the THz wavelength but larger than the infrared wavelength, one expects significantly larger attenuation in the infrared compared with the THz range. For fog, the attenuation in the THz range is given by

$$\alpha_{fog} = 0.1820 \times 10^{-3} \nu_{GHz} \mathrm{Im}\left(\widetilde{n}(\nu)\right) \quad [\mathrm{dB/m}] \tag{7}$$

where

$$\widetilde{n} = 3w/2m_w \frac{\varepsilon_w - 1}{\varepsilon_w + 2} \quad [\mathrm{ppm}] \tag{8}$$

is the complex refractive index of liquid water, w is the mass per volume of the water vapor droplets in units of g/m^3, m_w is the mass density of water in units of g/cm^3, and ε_w is the permittivity of liquid water given by the double Debye model. Using both the ITU model for atmospheric attenuation by gases and Eqs. (7) and (8) for the attenuation by water droplets, Eq. (5) may be used to determine the received power.

Figure 7 shows the calculated received THz power as a function of frequency. The propagation distance is 100 m, and the aperture radii for the transmitter and receiver are 0.5 m. The atmospheric temperature is 17 °C. In the figure, the received power for clear weather with 40% relative humidity (RH), corresponding to 5.78 g/m^3 water vapor density, is compared with clear weather with 100% RH (14.46 g/m^3 water vapor density). Even in the absence of fog droplets, the high relative humidity, which is required for fog formation, impacts the available THz frequency band for THzPB. Specifically, while frequencies close to 100 GHz experience only a small change in received power, frequencies close to 300 GHz exhibit decreases in power of approximately 10%. The additional attenuation due to airborne fog droplets strongly impacts the received powers. However, even at the highest range of fog droplet content (10 g/m^3), enough received power persists below 100 GHz to enable THzPB. In comparison, the attenuation at visible and infrared frequencies is even more severe. The visibility at 632 nm is defined as the distance at which 2% of the visible light is transmitted. For fog mass densities of 1, 5, and 10 g/m^3, the corresponding visibilities [30] are 16, 3.2, and 1.6 m, respectively. Under fog conditions, THzPB is still feasible, while a LPB system would be inoperable. For dust and fog airborne particulates, the contrast in atmospheric attenuation between near-infrared and THz attenuation is striking: As with wireless communication systems [20, 21, 28, 31], dust and fog can essentially block infrared beam propagation, while comparatively speaking, THz beam propagation is still possible over distances of at least 100 m.

Substantial attenuation can occur when the sizes of airborne particulates, such as rain droplets, sleet, and snow are comparable with the wavelength of the THz radiation [21, 32]. Raindrops, which are typically in the millimeter size range, are no longer "small" compared with the THz wavelength resulting in significant scattering and attenuation of THz radiation compared with dust and fog airborne particulates.

For rain, sleet, and snow calculations, the total atmospheric attenuation is given by $\alpha = \alpha_{ITU} + \alpha_{Mie}$, where $\alpha_{ITU}$is the attenuation due to atmospheric gas absorption calculated using the ITU model and α_{Mie} is the attenuation due to Mie scattering from airborne particulates. The power attenuation (dB/km) due to particulates is given by [22].

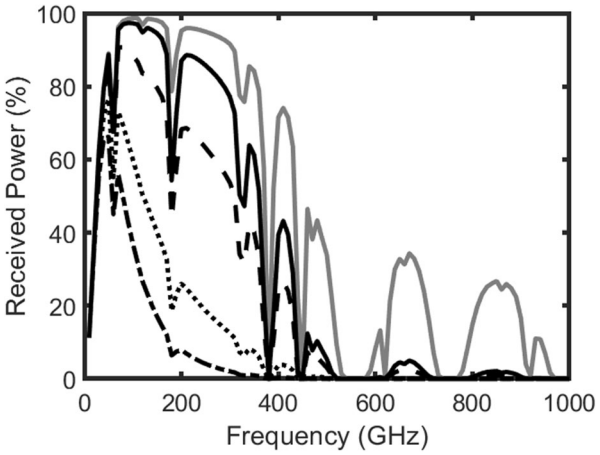

Fig. 7 Received power as a function of frequency through 100 m of various atmospheric conditions. For all curves, the temperature is 17 °C and the apertures are 0.5 m in radius. The gray curve corresponds to clear weather and 5.78 g/m^3 water vapor (40% relative humidity). The sold black line corresponds to clear weather conditions and 14.46 g/m^3 water vapor (100% relative humidity). The dashed, dotted, and dash-dot lines correspond to 14.46 g/m^3 water vapor with 1 g/m^3, 5 g/m^3, and 10 g/m^3 fog droplet content, respectively

$$\alpha_{Mie} = 4.343 \times 10^3 \int_{D_o}^{\infty} Q(D, \lambda, n) N(D)\, dD \tag{9}$$

where D_o is the minimum diameter, λ is the THz wavelength, n is the complex refractive index of the scattering medium, D is the particle diameter, and $N(D)$ is the particle number density distribution. The attenuation cross-section, $Q(D, \lambda, n)$, takes the form

$$Q(D, \lambda, n) = \frac{\lambda^2}{2\pi} \sum_{m=1}^{\infty} (2m+1) \mathrm{Re}(a_m + b_m) \tag{10}$$

The Mie coefficients, a_m and b_m, are parameters that depend on the refractive index and size parameter of the scatterers [28].

For rain, the Marshall-Palmer particle size distribution [22],

$$N(D) = 8000 e^{-4.1 D R^{-0.21}} \tag{11}$$

where R is the rain rate, is used to evaluate Eq. (9). Figure 8 shows received THz power versus frequency through 100 m of rain. These curves are generated using Eq. (5) and the total atmospheric attenuation $\alpha = \alpha_{ITU} + \alpha_{Mie}$. In the THz range, the attenuation due to rain adds a constant attenuation to the received power above ~ 100 GHz. This is consistent with the THz spectral dependence of the Mie scattering for rain [22], which exhibits small attenuation below ~ 100 GHz and roughly constant attenuation from 150 to 1000 GHz. Consequently, the best frequency range for THzPB in the presence of rain is determined by the atmospheric gas absorbance spectra, while the maximum range for THzPB is determined by the rain rate.

The calculation for sleet is similar to that of rain except the Polyakov-Shifrin particle size distribution [22].

$$N(D) = 11750 R^{-0.29} D^2 e^{-4.87 R^{-0.2}} \tag{12}$$

is used to evaluate Eq. (9), where R is the equivalent rain rate. Figure 9 shows the received THz power through sleet as a function of frequency. Note the lower specific attenuation for sleet compared with rain for identical equivalent rain rates. This can be understood as a result of a lower permittivity for ice compared with liquid water. In comparing Fig. 8 and Fig. 9, for the same equivalent rain rate, sleet has a smaller impact on THzPB than rain.

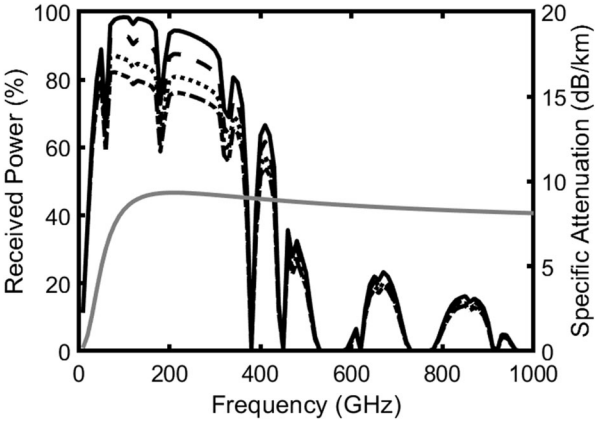

Fig. 8 Percent received power relative to transmitter power through 100 m of rain. Atmosphere conditions correspond to an atmospheric pressure of 1013.25 hPa, temperature of T = 288 K, and water vapor density of 7.5 g/m^3. Curves top to bottom correspond to no rain (solid black) and equivalent rain rates of 2 mm/h (dashed), 6 mm/h (dotted), and 10 mm/h (dash-dot). The effective radii of the transmitter and receiver are assumed to be 0.5 m. The gray curve corresponds to the specific attenuation of sleet for an equivalent rain rate of 10 mm/h

Finally, the calculation for snow is similar to that of rain except the Gunn-Marshall particle size distribution [22].

$$N(D) = 3800R^{-0.87}e^{-25.5DR^{-0.46}} \tag{13}$$

is used to evaluate Eq. (9). Figure 10 shows the specific attenuation and received power through snow as a function of frequency. The equivalent rain rates for these snow conditions is fixed at 2 mm/h (experimental measurements of THz attenuation through snow include Refs. [33, 34]). Clearly, the attenuation due to snow strongly depends on the liquid water content

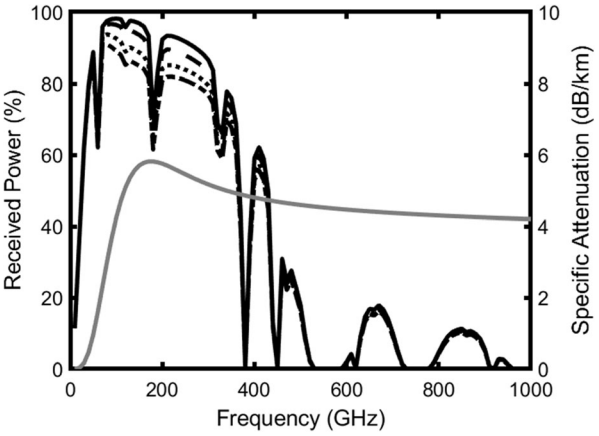

Fig. 9 Percent received power through sleet relative to transmitter power at a distance of 100 m. Atmosphere conditions correspond to an atmospheric pressure of 1013.25 hPa, temperature of T = 273 K, and water vapor density of 7.5 g/m^3. Curves top to bottom correspond to no sleet (solid black) and sleet with equivalent rain rates of 2 mm/h (dashed), 6 mm/h (dotted), and 10 mm/h (dash-dot). The effective radiuses of the transmitter and receiver are assumed to be 0.5 m. The gray curve corresponds to the specific attenuation of sleet for an equivalent rain rate of 10 mm/h

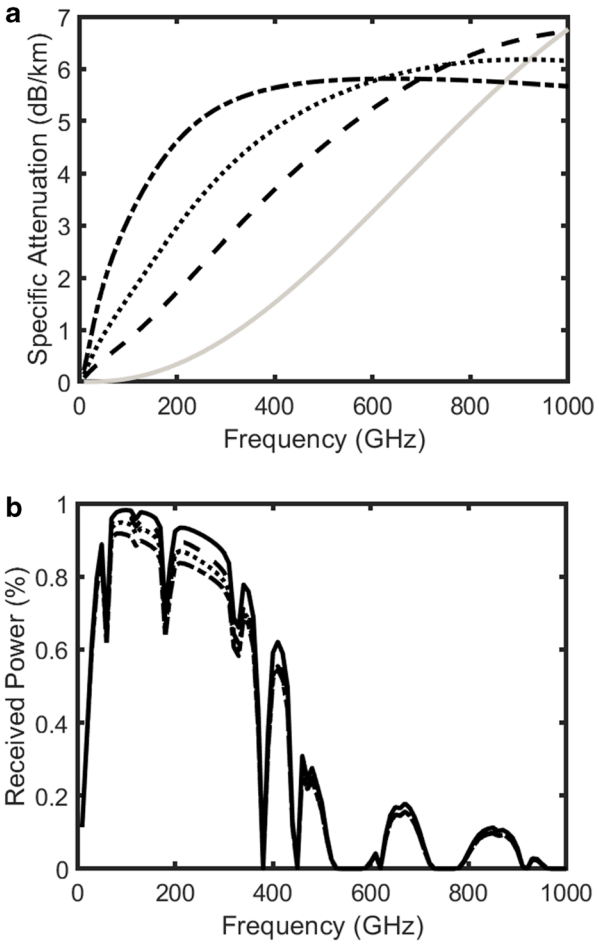

Fig. 10 **a** Comparison of specific power attenuation at 0 °C due to dry (gray line) and wet snow aggregates of 20% (dash-dot), 10% (dotted line), and 5% (dashed line) LWC (adapted from Fig. 2b of Ref. [22]). **b** Percent received power through snow relative to transmitter power at a distance of 100 m. Atmosphere conditions correspond to an atmospheric pressure of 1013.25 hPa, temperature of T =273 K, and water vapor density of 7.5 g/m^3. Curves top to bottom correspond to no snow (solid black) and snow for 5% (dashed), 10% (dotted), and 20% (dash-dot) liquid water content of the snow. For each liquid water content, the equivalent rain rate for the snow is fixed at 2 mm/h. The effective radiuses of the transmitter and receiver are assumed to be 0.5 m

(LWC) of the snow aggregates. In the presence of dry snow, there is very little change in the received THz power at 100 m (curve not shown in Fig. 10b). As would be expected, the received THz power decreases slightly as the LWC of the aggregates increases. In comparing the 2 mm/h rain curve from Fig. 8 with the snow aggregate curves from Fig. 10, as the LWC of the snow aggregates increases, the predicted change of the received power relative to a clear atmosphere approaches that of rain.

In comparing the rain performance of atmospheric transmission for THzPB to that for LPB at 1.5 μm, one can utilize simultaneously measured attenuation rates for THz radiation and infrared radiation [27]. Under identical rain conditions and equal beam diameters, a 625-GHz beam signal suffers slightly higher attenuation compared with a 1.5-μm infrared beam due to the slightly larger extinction cross-section of raindrops in the THz band. Since the specific attenuation for rain is roughly frequency independent from 100 to 1000 GHz (Fig. 8), there is a slight advantage in using LPB compared with THzPB in the presence of rain. However, the effects of winter weather on the THz versus infrared beams is more complicated. Specifically, in the near-infrared, the specific attenuation due to winter weather increases relative to that of rain, while the introduction of either sleet or snow can either increase or decrease the THz

specific attenuation relative to rain [22] depending on the exact THz frequency. As shown in [22], the specific attenuation in a rain rate of 2 mm/h is roughly constant at ~3.1 dB/km from 0.2 to 1 THz. Comparing this value of specific attenuation to those of winter weather conditions in Fig. 10, the presence of winter weather tends to increase the attenuation relative to an equivalent rain except for sufficiently low (i.e. < 400 GHz) THz frequencies and relatively dry snow (LWC < 10%). Below ~400 GHz, a decrease in the liquid water content of snow (from wet to dry snow) decreases the THz specific attenuation due to airborne particulates relative to rain, while infrared specific attenuation increases roughly by a factor of 3.6 (at a snow rate of 4 mm/h) according to ITU guidelines [35]. Since THzPB and LPB should have comparable specific attenuation in the presence of rain, lower frequency THzPB could have an advantage over LPB under winter weather conditions.

Air turbulence is another atmospheric condition that strongly affects power beaming. Air turbulence is typically due to localized heating of the air that results in a temporal and spatial dependent real refractive index. Air turbulence (and scintillations related to air turbulence) have a much stronger influence on infrared light compared with THz radiation [36]. Scintillation effects are dominated by the optical path length through the turbulent air relative to the electromagnetic wavelength. The refractive indices of air in the infrared and THz ranges are comparable, and so, since the infrared electromagnetic wavelength (roughly 1.5 μm) is much smaller than the THz electromagnetic wavelength (roughly 600 μm at 500 GHz), scintillation effects are much more prevalent in the near-infrared band. Based on previous studies [21], under identical turbulence conditions, an infrared laser beam attenuates more than a THz signal. Specifically, the THz signal shows almost no degradation [21]. For airflows comparable with the speed of hurricanes and temperature enhancements of several tens of degrees Kelvin, the attenuation of the THz signal stays below a tenth of a dB/m [21].

4 Discussion

4.1 THz Rectifying Diodes

The analysis given in Sect. 3 assumed that the conversion efficiency of the THz receiver is 100%. While efficient converters operating at 1550 nm (45% optical to electrical conversion efficiency) [37] and in the microwave range (~90% efficiency) [13] are available, demonstrated efficiencies are much lower in the THz range. The success of development of a wireless power transfer system at THz frequencies will require development and advances of rectifying diodes, which can operate at these frequencies [10]. THz power beaming at 303 GHz [13] demonstrated a conversion efficiency of ~2%. The major technology gap in the development of THzPB is the low efficiency of THz rectifying diodes. It is important to note that for a 100-m distance and the power beaming requirements described in the previous section, this 303-GHz operational frequency would be useful if the diode efficiency could be improved.

One can estimate the required THz source power for a 100-m target distance. Assuming a received target power of 10 W at 303 GHz, the 90% transmission through the clear atmosphere coupled with a 2% conversion efficiency of THz power into electrical power implies that a ~ 560-W source is required. Not only are the power requirements of the source relatively large

due to the inefficiency of power conversion but also the intensity of the source exceeds the MPE levels given by Table 1. In the presence of adverse weather such as dust and fog, there is an advantage in shifting THzPB operation to lower frequencies. For example, at 94 GHz, conversion efficiencies of approximately 40% have been demonstrated [38, 39].

4.2 Dual Channel THz Beam Powering/Communications

In both the THz frequency range and the near-infrared frequency range, one can integrate power beaming and wireless communication into the same modality. Specifically, a dual channel approach for integrating power beaming with wireless communications can be exploited: one frequency for power beaming and the second frequency for communication. As with power beaming, the wireless communication channel could be either in the near-infrared or in the THz range. However, analogous to the analysis above for beam propagation through adverse weather conditions, a THz wireless link has the advantage over an infrared link in adverse weather.

Intrinsic atmospheric attenuation of THz radiation, while limiting the maximum propagation distance and range of THzPB, could also be a benefit for secure THz wireless links. Atmospheric absorption controls signal spreading and limits the detection range of the THz wireless link. As an example of this approach in wireless communications, attenuation in the infrared band (5–7 μm) can be used for secure wireless communications [40].

5 Comparison of Microwave, THz, and Laser Power Beaming

Microwave, THz, and laser power beaming each have their unique advantages. To identify which is optimal in a particular instance, it is important to specify target distances, aperture sizes, and weather conditions. For a fixed aperture size of the transmitter and receiver, the maximum range for power beaming is limited by two factors: the spreading of the propagating beam due to diffraction (i.e. free space damping) and the atmospheric attenuation. The approximate range due to diffraction is determined by the Rayleigh range. For an aperture radius of 0.5 m, the Rayleigh ranges (Eq. (2)) for the microwave (2.45 GHz), THz (300 GHz), and infrared (1500 nm wavelength) beams are given by 2.8 m, 340 m, and 228 km, respectively. Clearly, for long-range power beaming (> 1 km), near-infrared power beaming is the preferred methodology. Microwave power beaming is only practical for relatively short distances. For longer distances, the power in the microwave source would need to be significantly increased resulting in a significant safety hazard in the beam path to compensate for the spreading of the power over a larger area due to diffraction.

In the THz range, as the link distance increases in clear weather conditions, one can compensate for spreading of the beam by increasing the frequency. While increasing the THz frequency can counteract the effects of diffraction, atmospheric attenuation by water vapor will limit the maximum effective range for THzPB. In clear weather conditions, infrared power beaming will be superior to THz power beaming.

When the airborne particulates are in the 1–50 μm range, scattering and subsequent attenuation are weaker in the THz frequency range compared with the near-infrared. This reduced attenuation in the THz band is due to relatively small particulate sizes compared with the electromagnetic wavelength. In the presence of fog and dust, laser power beaming becomes inoperable, while THzPB is still feasible for distances of ~ 100 m. In the presence

of rain, the significantly larger drop sizes (~ 1 mm) attenuate both infrared and THz frequencies roughly equally. However, under winter weather conditions, the effects on THzPB and LPB are more complicated. The specific attenuation under winter weather conditions increases relative to rain for both LPB and THzPB above ~ 400 GHz. As the fraction of liquid water in snow particulates decreases, the specific attenuation due to the airborne particulates can decrease in the lower frequency THz range, while the specific attenuation in the near-infrared range increases. In the presence of adverse weather conditions most notably fog, dust, and air turbulence, THzPB exhibits longer maximum link distances and potentially superior performance compared with LPB.

Any advantages in implementing THzPB depend strongly on the development of efficient rectifying diodes in THz frequencies. Currently, the conversion efficiencies are in the ~ 2% range at 303 GHz. Typical photovoltaic receivers for LPB are about 45% efficient. If modest power beaming distances (~ 100 m) are required in either clear weather or adverse weather conditions, THzPB systems operating at 94 GHz may be viable with current technology since the conversion efficiency can be as high as ~ 40%.

Funding Information This work is supported by the US Army Combat Capabilities Development Command (CCDC) Armaments Center at Picatinny Arsenal.

References

1. N. Shinohara, Proc. IEEE 101 (6), 1448-1463 (2013)
2. W.C Brown, IEEE Transactions on Microwave Theory and Techniques, MTT-32 (9), 1230-1242 (1984)
3. J.J. Schlesak, in *Microwave Symposium Digest, IEEE MTT-S International,* (New York, 1988)
4. M. Nariman, IEEE Transactions on Microwave Theory and Techniques 64 (8), 2664 – 2677 (2016)
5. L. Summerer, Concepts for Wireless Energy Transmission via Laser. (European Space Agency, 2009), https://www.esa.int/gsp/ACT/doc/POW/ACT-RPR-NRG-2009-SPS-ICSOS-concepts-for-laser-WPT.pdf. Accessed 15 January 2020
6. NASA, LaserMotive Wins $900,000 from NASA in Space Elevator Games. *(NASA,* 2009), https://www.nasa.gov/centers/dryden/status_reports/power_beam.html . Accessed 15 January 2020
7. R. Whittle, How It Works: Laser Beaming Recharges UAV in Flight. (Popular Mechanics, 2012) https://www.popularmechanics.com/flight/drones/a7966/how-it-works-laser-beaming-recharges-uav-in-flight-11091133/. Accessed 15 January 2020
8. S.S. Dhillon, M.S. Vitiello, E.H. Linfield, A.G. Davies, M.C. Hoffmann, J. Booske, C. Paoloni, M. Gensch, P. Weightman, G.P. Williams, E. Castro-Camus, D.R.S. Cumming, F. Simoens, I. Escorcia-Carranza, J. Grant, S. Lucyszyn, M. Kuwata-Gonokami, K. Konishi, M. Koch, C.A. Schmuttenmaer, T.L. Cocker, R. Huber, A.G. Markelz, Z.D. Taylor, V.P. Wallace, J. Axel Zeitler, J. Sibik, T.M. Korter, B. Ellison, S. Rea, P. Goldsmith, K.B. Cooper, R. Appleby, D. Pardo, P.G. Huggard, V. Krozer, H. Shams, M. Fice, C. Renaud, A. Seeds, A. Stohr, M. Naftaly, N. Ridler, R. Clarke, J.E. Cunningham, and M.B. Johnston, Journal of Physics D: Applied Physics (2017) https://doi.org/10.1088/1361-6463/50/4/043001
9. M.Y. Glyavin, G.G. Denisov, V.E. Zapevalov, A.N. Kuftin, A.G. Luchinin, V.N. Manuilov, M.V. Morozkin, A.S. Sedov, and A.V. Chirkov, Journal of Communications Technology and Electronics (2014) https://doi.org/10.1134/S1064226914080075
10. K. Bhatt, Indian Journal of Pure and Applied Physics 53, 827-837 (2015)
11. K. Moon, J.H. Shin, I.M. Lee, D.W. Park, E.S. Lee, and K.H. Park, Nanotechnology (2018) https://doi.org/10.1088/1361-6528/aae130
12. S. Shriwastava and C.C. Tripathi, Journal of Electronic Materials (2019) https://doi.org/10.1007/s11664-018-06887-9
13. S. Mizojiri, K. Shimamura, M. Fukunari, S. Minakawa, S. Yokota, Y. Yamaguchi, Y. Tatematsu, and T. Saito, IEEE Microwave and Wireless Components Letters (2018) https://doi.org/10.1109/LMWC.2018.2860248
14. L. Rizzo, K.J. Duncan, J.L. Zunino, and J.F. Federici, Journal of Laser Applications (2018) https://doi.org/10.2351/1.5042166

15. American National Standards Institute. *Z136.1-2014 American National Standard for Safe Use of Lasers*. 2014.
16. IEEE, *IEEE Standard for Safety Levels with Respect to Human Exposure to Radio Frequency Electromagnetic Fields, 3 kHz to 300 GHz*. 2006, IEEE: New York, NY.
17. IEEE, *IEEE Recommended Practice for Measurements and Computations of Radio Frequency Electromagnetic Fields With Respect to Human Exposure to Such Fields, 100 kHz–300 GHz*. 2002, IEEE: New York, NY.
18. B.E.A. Saleh, M. C. Teich, Fundamentals of Photonics, (Wiley-Interscience, United States, 1991)
19. J. Federici, L. Moeller, K. Su, in Handbook of Terahertz Technology for Imaging, Sensing and Communictions, ed. By D. Saeedkia (Woodhead Publishing, Cambridge, 2013)
20. J. Federici and L. Moeller, Journal of Applied Physics (2010) https://doi.org/10.1063/1.3386413
21. J.F. Federici, J. Ma, and L. Moeller, Nano Communication Networks (2016) https://doi.org/10.1016/j.nancom.2016.07.006
22. D. Renaud and J.F. Federici, Journal of infrared, Millimeter, and Terahertz Waves 40 (8), 868-877 (2019)
23. International Telecommunications Union. *Recommendation ITU-R P.676-11 : Attenuation by Atmospheric Gases* (2016)
24. G.A. Siles, J.M. Riera, and P. García-Del-Pino, IEEE Antennas and Propagation Magazine, (2015) https://doi.org/10.1109/MAP.2015.2401796
25. Y. Yang, M. Mandehgar, and D.R. Grischkowsky, IEEE Photonics Technology Letters (2015) https://doi.org/10.1109/LPT.2014.2375795
26. D.M. Slocum, E.J. Slingerland, R.H. Giles, and T.M. Goyette, Journal of Quantitative Spectroscopy and Radiative Transfer (2013) https://doi.org/10.1016/j.jqsrt.2013.04.022
27. J. Ma, F. Vorrius, L. Lamb, L. Moeller, and J.F. Federici, Journal of Infrared, Millimeter, and Terahertz Waves (2015) https://doi.org/10.1007/s10762-015-0200-6
28. K. Su, L. Moeller, R.B. Barat, and J.F. Federici, J. Opt. Soc. Am. A 29 (11), 2360-2366 (2012)
29. H.J. Liebe and G.A. Hufford, IEEE Transactions on Antennas and Propagation (1989) https://doi.org/10.1109/8.45106
30. Y. Golovachev, A. Etinger, G.A. Pinhasi, and Y. Pinhasi, Journal of Applied Physics (2019) https://doi.org/10.1063/1.5083711
31. K. Su, L. Moeller, R.B. Barat, and J.F. Federici, J. Opt. Soc. Am. A (2012) https://doi.org/10.1364/JOSAA.29.000179
32. A. Bandyopadhyay, A. Sengupta, R.B. Barat, D.E. Gary, J.F. Federici, M. Chen, and D.B. Tanner, International Journal of Infrared and Millimeter Waves (2007) https://doi.org/10.1007/s10762-007-9276-y
33. E.B. Moon, T.I. Jeon, and D.R. Grischkowsky, IEEE Transactions on Terahertz Science and Technology **5** (5), 742-750 (2015)
34. J. Ma, J. Adelberg, R. Shrestha, L. Moeller, and D. M. Mittleman, Journal of Infrared, Millimeter, and Terahertz Waves 39 (6), 505-508 (2018)
35. International Telecommunications Union, Recommendation ITU-R P.1817-1. *Propagation data required for the design of terrestrial free-space optical links* (2012)
36. J. Ma, L. Moeller, and J.F. Federici, Journal of Infrared, Millimeter, and Terahertz Waves (2015) https://doi.org/10.1007/s10762-014-0121-9
37. W.W. Jayanta Mukherjee, Holger Hartje, Frank Steinsiek, Matthew Perren, Stephen J. Sweeney (2013) https://doi.org/10.1109/PVSC.2013.6744326
38. H.K. Chiou and I.S. Chen, IEEE Transactions on Microwave Theory and Techniques (2010) 0.1109/TMTT.2010.2086350
39. K.M.K. Komurasaki, W. Hatakeyama, Y. Okamoto, S. Minakawa, M. Suzuki, K. Shimamura, A. Mizushima, K. Fujiwara, and H. Yamaoka (2017) https://doi.org/10.1109/WPT.2017.7953902
40. D. Kedar and S. Arnon, IEEE Communications Magazine, 42 (5), S2-S7 (2004)